Complex Spatial Patterns on Planar Continua

Gemunu H. Gunaratne
Department of Physics, The University of Houston, Houston, Texas 77204
(Received 5 March 1993)

The Landau-Ginzburg equations used to describe periodic spatial patterns in two dimensions are extended to a set of spatiotemporal equations. The extension is determined by the requirement that the equations of motion commute with translations, reflections, and rotations in the plane. This simple model produces a variety of complex structures similar to those observed in chemical reactions, ferrofluids, Rayleigh-Bénard convection, and magnetic bubble materials.

PACS numbers: 47.10.+g, 47.20.Ky

Many natural patterns such as animal coats and beehives consist of arrays that are very regular (often hexagonal or striped) on the small scale, but are highly irregular on a large scale. Qualitatively similar structures have been observed recently in experiments performed on systems as diverse as chemical reactions [1], ferrofluids [2], and magnetic bubble material [3]. This Letter is an attempt to understand the apparent universality and determine the ingredients required to produce such structures.

Let us first review the theory for periodic patterns. We focus on isotropic, extended (i.e., the boundaries are far away) domains. Bifurcations from the uniform state typically lead to patterns with a unique length scale. The structures that tile the plane are hexagons, stripes, and squares. The patterns $U(\mathbf{x},t)$ most often seen in experimental and natural systems are hexagons and stripes (or rolls) which can be expanded in a *hexagonal planform* [4] as

$$U(\mathbf{x},t)=A_1(x,t)e^{i\mathbf{k}_1\cdot\mathbf{x}}+A_2(x,t)e^{i\mathbf{k}_2\cdot\mathbf{x}}+A_3(\mathbf{x},t)e^{i\mathbf{k}_3\cdot\mathbf{x}}, \tag{1}$$

where $\mathbf{k}_i$ are a set of hexagonal basis vectors [5]

$$\mathbf{k}_1=k_0\mathbf{j},\quad \mathbf{k}_2=k_0\left(\frac{\sqrt{3}}{2}\mathbf{i}-\frac{1}{2}\mathbf{j}\right),\quad \mathbf{k}_3=k_0\left(-\frac{\sqrt{3}}{2}\mathbf{i}-\frac{1}{2}\mathbf{j}\right), \tag{2}$$

and $A_n(\mathbf{x},t)$ are slowly varying complex functions called the envelope functions [6]. Here $U(\mathbf{x},t)$ is some field that characterizes the pattern. For chemical systems it could be the difference between the local concentration of a species and its mean value over the plane, while for convective patterns it could denote the fluid surface velocity. The existence and stability of hexagonal and striped arrays can be determined using the *Landau-Ginzburg equations* [7,8],

$$\begin{aligned}\dot{A}_1&=f_1(\mathbf{x},t)=\mu A_1+\alpha\bar{A}_2\bar{A}_3-(|A_1|^2+\rho|A_2|^2+\rho|A_3|^2)A_1,\\ \dot{A}_2&=f_s(\mathbf{x},t)=\mu A_2+\alpha\bar{A}_3\bar{A}_1-(|A_2|^2+\rho|A_3|^2+\rho|A_1|^2)A_2,\\ \dot{A}_3&=f_3(\mathbf{x},t)=\mu A_3+\alpha\bar{A}_1\bar{A}_2-(|A_3|^2+\rho|A_1|^2+\rho|A_2|^2)A_3,\end{aligned} \tag{3}$$

parametrized by real numbers μ, α, and ρ. Here $\dot{A}$ and $\bar{A}$ denote the time derivative and the complex conjugate of A, respectively. The envelope functions for uniform stripes parallel to the x axis are $A_1=$const, $A_2=A_3=0$, while those for a uniform array of hexagons are $A_1=A_2=A_3=$const. Figure 1 summarizes the linear stability of hexagons and stripes. We note that mixed states (which correspond to $A_2=A_3\neq A_1$) can exist but are unstable in this model [8].

The Landau-Ginzburg equations are based only on the symmetries of the interface and thus describe the patterns on a large class of (essentially) two-dimensional continua. For example, the fact that $\mathbf{k}_1$, $\mathbf{k}_2$, and $\mathbf{k}_3$ can be permuted in (1) implies that Eqs. (3) are invariant under any permutation of indices. The reflection symmetry requires that the dynamics [of $U(\mathbf{x},t)$] commute with the reflection κ about the y axis; i.e., given a pattern $U(\mathbf{x},t_0)$, the evolution of the reflected pattern $V(\mathbf{x},t_0)=U(\kappa^{-1}\mathbf{x},t_0)$ [with envelope functions $A_n(\kappa^{-1}\mathbf{x},t_0)$] has to satisfy

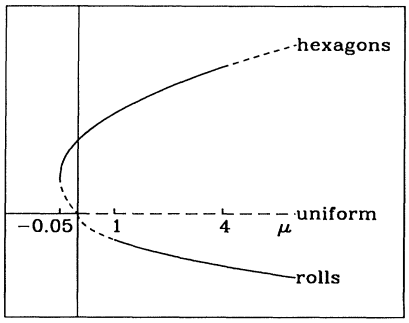

FIG. 1. The stability domains of the uniform state, hexagons, and rolls in the Landau-Ginzburg equations. Solid lines correspond to stable states while dashed lines correspond to unstable states. The vertical axis measures the amplitude of the pattern. The parameters α and ρ are chosen to be 1 and 2, respectively, in all calculations presented.

0031-9007/93/71(9)/1367(4)$06.00

$V(\mathbf{x},t)=U(\kappa^{-1}\mathbf{x},t)$ for $t>t_0$. Further, the necessity for the dynamics to commute with reflection about the x axis demands μ, α, and ρ to be real. Finally, translation by $\mathbf{x}_0$ leads to a pattern $U(\tau^{-1}\mathbf{x},t_0)$ described by the envelope functions $A_n(\tau^{-1}\mathbf{x},t_0)e^{-i\mathbf{k}_n\cdot\mathbf{x}_0}$ $(n=1,2,3)$. The necessity for the dynamics to commute with translations restricts the form of the coupling terms (e.g., the term $\bar{A}_2\bar{A}_3$ in the first equation).

Figure 2 shows an extended pattern that develops in a chlorite-iodide-malonic acid reaction in a thin disk reactor [1]. The reaction, known as the CIMA reaction, occurs in a gel that is in contact with continuously refreshed chemical reservoirs. The system has undergone a Turing bifurcation that leads to the selection of a natural length scale (over which the rate of reaction varies). The colors of the oxidized and nonoxidized regions are different leading to the observed patterns. The parameter values (of Fig. 2) correspond to stable stripes, and it is seen that local patches of the pattern are indeed striped (pointing in arbitrary directions). The uniform patches are arranged in a very complex mosaic, primarily due to the inhomogeneity of the initial state. In addition, there are several *defects,* i.e., points at which the direction of the rolls is not defined uniquely. Qualitatively similar patterns have been observed in experiments on ferrofluids [2], Rayleigh-Bénard convection [9], magnetic bubble materials [3], and in mathematical models [10,11]. The commonality of the observed patterns in diverse experiments (as well as animal coats?) demands a model independent description.

The absence of spatial coupling in (3) implies that each point evolves independent of its neighbor. However, the smoothness of the experimental pattern (except at the defects) suggests that spatial derivatives need to be added to the description. We determine the form of the spatial derivatives by requiring that the dynamics commute with invariants of rigid body motions. In particular, we demand that the equations of motion commute with arbitrary rotations. That is, given a pattern $U(\mathbf{x},t_0)$ and any *rotated pattern* $V(\mathbf{x},t_0)=U(\mathcal{R}^{-1}\mathbf{x},t_0)$, the dynamics has to imply that $V(\mathbf{x},t)=U(\mathcal{R}^{-1}\mathbf{x},t)$ for all subsequent times. The required condition can be deduced by analyzing a uniform array of rolls. Rolls parallel to the x axis are given by $U_0=a_1e^{i\mathbf{k}_1\cdot\mathbf{x}}$, while rolls oriented at an angle θ to the x axis can be written as $U_\theta=a_1e^{i\mathbf{k}_1(\theta)\cdot\mathbf{x}}$, with $\mathbf{k}_1(\theta)=(k_0\sin\theta)\mathbf{i}+(k_0\cos\theta)\mathbf{j}$. Rotational invariance implies that a_1 is independent of θ. The solution U_θ can be expanded in the original basis $(\mathbf{k}_1,\mathbf{k}_2,\mathbf{k}_3)$ using envelope functions

$$A_1=a_1e^{i\Delta\mathbf{k}_1\cdot\mathbf{x}},\quad A_2=A_3=0, \tag{4}$$

with $\Delta\mathbf{k}_1=\mathbf{k}_1(\theta)-\mathbf{k}_1=k_0\sin\theta\mathbf{i}-k_0(1-\cos\theta)\mathbf{j}$. What is needed then is a combination $\Box_1$ of spatial derivatives that will satisfy the condition $\Box_1e^{i\Delta\mathbf{k}_1\cdot\mathbf{x}}=0$. It is easy to check that

$$\Box_1=\left(\hat{\mathbf{k}}_1\cdot\nabla-\frac{i}{2k_0}\nabla^2\right) \tag{5}$$

is the simplest such combination. Defining $\Delta\mathbf{k}_2$, $\Delta\mathbf{k}_3$, $\Box_2$, and $\Box_3$ analogously, we see that for $n=1,2,3$

$$\Box_ne^{i\Delta\mathbf{k}_n\cdot\mathbf{x}}=0. \tag{6}$$

We are thus motivated to introduce a spatially dependent extension of the Landau-Ginzburg equations,

$$\begin{aligned}\partial_tA_1&=f_1(\mathbf{x},t)+\gamma\Box_1^2A_1+\nu\bar{\Box}_2\bar{A}_2\bar{\Box}_3\bar{A}_3,\\ \partial_tA_2&=f_2(\mathbf{x},t)+\gamma\Box_2^2A_2+\nu\bar{\Box}_3\bar{A}_3\bar{\Box}_1\bar{A}_1,\\ \partial_tA_3&=f_3(\mathbf{x},t)+\gamma\Box_3^2A_3+\nu\bar{\Box}_1\bar{A}_1\bar{\Box}_2\bar{A}_2,\end{aligned} \tag{7}$$

$\bar{\Box}_n$ being the complex conjugate of $\Box_n$. For the rest of the Letter the model (7) (with parameters γ and ν) will be referred to as the $\gamma\nu$ model.

Some comments are in order. Given a pattern $U(\mathbf{x},t)$, the envelope functions for the rotated pattern $U(\mathcal{R}^{-1}\mathbf{x},t)$ are $A_n(\mathcal{R}^{-1}\mathbf{x},t)e^{i\Delta\mathbf{k}_n\cdot\mathbf{x}}$ [12]. It follows from (6) that the dynamics given by the $\gamma\nu$ model commutes with arbitrary rotations, as was required all along. Second, terms such as $i\Box_1A_1$ and $i(\bar{A}_2\bar{\Box}_3\bar{A}_3+\bar{A}_3\bar{\Box}_2\bar{A}_2)$ can be added to the first of Eqs. (7) (with corresponding terms in the other equations) without violating the symmetries. However, they can be scaled away by a suitable redefinition of k_0 and are thus ignored. Finally observe that when $\nu=0$, (7) can be derived from a variational principle, $\partial_tA_k=-\delta(\int dx\,dy\,\mathcal{L})/\delta\bar{A}_k$ with

$$\begin{aligned}\mathcal{L}=&-\mu\sum_{n=1}^{3}|A_n|^2-\alpha(A_1A_2A_3+\bar{A}_1\bar{A}_2\bar{A}_3)\\&+\frac{1}{2}\sum_{n=1}^{3}|A_n|^4+\rho\sum_{n\neq m}|A_n|^2|A_m|^2+\gamma\sum_{n=1}^{3}|\Box_nA_n|^2.\end{aligned} \tag{8}$$

Thus the last terms in (7) are required to capture nonvariational effects on pattern formation.

As in Eq. (3), hexagons and rolls are stable in the $\gamma\nu$ model. However, unlike (3) there is a band of parameters (much like the Eckhaus band) within which the mixed states are stable. These correspond to rhombic

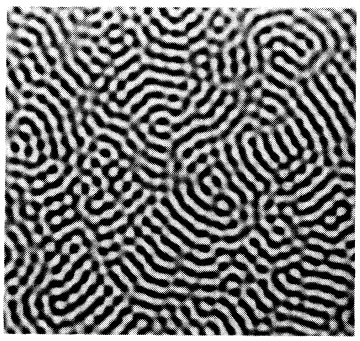

FIG. 2. A *chemically turbulent* pattern from the CIMA reaction (Ouyang and Swinney). The dark (light) regions of the figure correspond to the reduced (oxidized) states of the system.

patterns of the interface which have been recently observed in the CIMA reaction [13] and in numerical models [14].

Equations similar in form to (7), but with $\Box_n$ approximated by $\hat{\mathbf{k}}_n \cdot \nabla$ have been introduced in Ref. [15]. Qualitative properties of uniform states such as the stability of hexagons and stripes, and the existence of rhombic arrays, will be identical in both models. The differences of the two models will be significant when the rotational invariance is important. For example, Eq. (7) will be crucial to the study of domain walls between stripes pointing in different directions. Since rotations are a continuous symmetry of the plane, approximations which do not preserve the symmetry exactly may lead to qualitatively incorrect patterns. In fact, numerically we find qualitative differences in the behavior of domain walls in the two models. One key suggestion of this work is that perturbation expansions of any microscopic model should be constructed to preserve the relevant symmetries.

The similarity of $\Box_n$ to the derivatives in the Newell-Whitehead-Segel model [6] suggests that multiple scale analysis may be used to get $\Box_n$. This is indeed the case. On carrying out the analysis to sufficiently high order we get the derivatives in the combination $\Box_n$. For the Swift-Hohenberg equation [11] one retains the combination $\Box_n$ at all orders beyond the fifth.

We next describe properties of the nonperiodic states. Unfortunately, very little analysis can be done for these complex states and we present results from the numerical integration of (7). The time evolution is done using the alternating direction implicit algorithm [16]. Each nonlinear term $N[A(\mathbf{x},t)]$ is expanded to linear order in $\delta A = A(\mathbf{x},t+\delta t) - A(\mathbf{x},t)$, thus linearizing the equations in $A(\mathbf{x},t+\delta t)$. The cross derivatives, such as $\partial^4 A_l / \partial x^2 \partial y^2$, are calculated explicitly. The results presented here are from the evolution of A_k's on a 32×32 lattice with periodic boundary conditions. The slow variables A_k are interpolated to a 128×128 lattice on which $U(\mathbf{x},t)$ is evaluated using (1). The domain is chosen to have a length of 4π in each direction and k_0 is 4.0. Each time step was 0.01 unit, and it was checked in several cases that smaller time steps do not change the conclusions.

Figure 3 shows a typical pattern from the numerical integration of a random initial state. Observe the qualitative similarity between Figs. 2 and 3. The parameters have been chosen so that only stripes (which by isotropy can point in any direction) are stable. It is seen that local patches develop into independent arrays of stripes. The domain sizes in the patterns increase with the *diffusion coefficient* γ. When the different domains run into each other, the isotropy allows for the rolls to bend at the boundary and join smoothly (as opposed to forming domain walls). In nonvariational systems (i.e., $\nu \neq 0$) the patterns do not appear to settle down; i.e., they are time dependent. Close to the onset of stripes (e.g., $\mu \sim 5$) the pattern is found to evolve relatively fast, while further away from the onset (e.g., $\mu \sim 10$) the evolution is very slow.

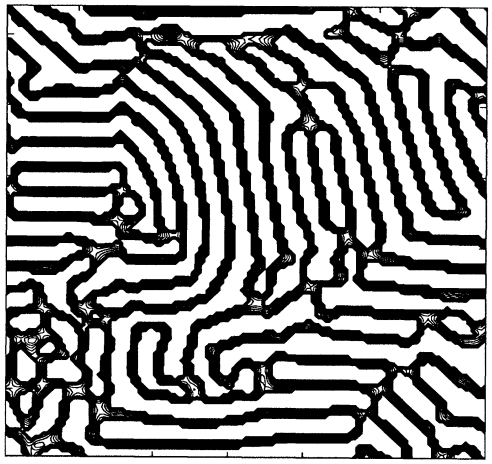

FIG. 3. The central contours of the pattern $U(\mathbf{x},t)$ resulting from the evolution of a random state by (7) with $k_0 = 4.0$, $\alpha = 1.0$, $\rho = 2.0$, $\gamma = 0.1$, $\mu = 6.0$, and $\nu = -0.19$. The domain is of length 4π in each direction and periodic boundary conditions are imposed. The interface $U(\mathbf{x},t)$ is constructed from (1). The pattern is time dependent, and does not appear to become stationary.

For parameters close to the onset of stripes (e.g., $\mu \approx 5$, $\gamma = 0.1$, and $\nu = -0.2$) the pattern can consist of hexagonal and striped regions that continually invade each other's domain. However, it appears that the structure eventually settles to one or the other periodic patterns. Qualitatively similar behavior has been observed in the CIMA reaction [1].

Figure 4 shows a structure resulting from the evolution of (7) in the absence of nonvariational terms (i.e., $\nu = 0$). In this case the patterns appear to be stationary, even though $U(\mathbf{x},t)$ exhibits small ($\sim 0.1\%$) fluctuations due to the finiteness of δt [17]. Further, the pattern appears to consist of distinct domains with sharper domain walls in between. The stripes in neighboring domains form an angle close to 120° with each other [18]. Similar qualitative properties are observed in patterns on magnetic bubbles and ferrofluids (both of which are conservative systems).

If $\Box_1$ is replaced by $\hat{\mathbf{k}}_1 \cdot \nabla$, the isotropy of the set of solutions will be broken and local set of rolls will align in certain preferred directions, producing more abrupt domain walls. The resulting patterns are qualitatively different from Figs. 3 and 4. The physics behind the model (7) is that local regions (whose size is determined by the diffusion length) form arrays of rolls. The isotropy of the dynamics allows for the bending of rolls at the boundaries leading to the observed smoothly varying patterns. Thus the complex structures (of Fig. 2, for example) are a consequence of the spatial extent of the domain and the inhomogeneity of the initial state. If one of the other symmetries is broken, then retaining the exact form of $\Box_n$ may not be necessary. For example, in rotating

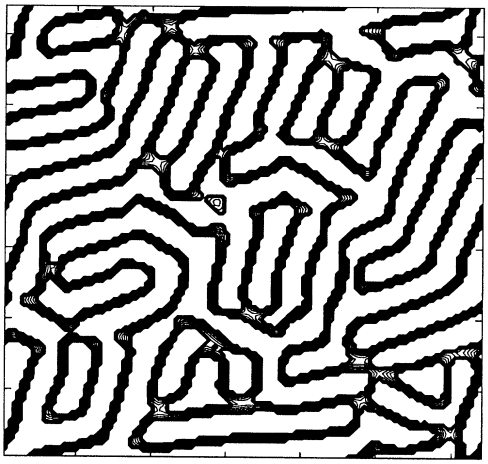

FIG. 4. The contours for a pattern $U(\mathbf{x},t)$ resulting from the evolution of a random state by (7) with the same parameters as in Fig. 3 except for $\mu=8.0$, $\gamma=0.2$, and $\nu=0$. The pattern appears to be stationary apart from small fluctuations due to the finiteness of δt. These fluctuations decrease when δt is reduced. Notice that the stripes in neighboring domains make an angle close to 120° with each other.

convection (where the reflection symmetry is absent) approximating $\Box_n$ by $\hat{\mathbf{k}}_n\cdot\nabla$ leads to structures qualitatively similar to experimental patterns [19].

Similarities seen in patterns forming in disparate experiments demand a model independent description. What we have proposed here is that spontaneous loss of translational invariance coupled with the invariance of the equations of motion under translations, rotations, and reflections lead to such patterns; see Figs. 3 and 4. Unlike complex Landau-Ginzburg equations [10] (which also show patterns like Fig. 4), model (7) preserves the symmetries of the physical system. The variational and nonvariational dynamics appear to lead to different behavior. The patterns in the variational model are stationary, and neighboring domains orient close to 120° from each other, reminiscent of structures on ferrofluids and magnetic bubbles. The patterns forming in the nonvariational model appear to be time dependent, and consist of curved domains similar to structures produced by the CIMA reaction. It is important to be able to prove these assertions from (7) and to determine which of them generalize to other models. It will also be of interest to determine if Eqs. (7) are consistent with the rotationally invariant Cross-Newell equations [18]. Finally, we would like to know if the form of $\Box_n$ follows from the generators of the symmetry group. If so, we will be able to deduce the form of the amplitude equations in other geometries (such as in systems with cylindrical symmetry).

It is a pleasure to thank Qi Ouyang and Harry Swinney for many fruitful discussions and for providing Fig. 2. I have also benefited from discussions with Martin Golubitsky, Mike Gorman, Alan Newell, and Ian Melbourne, This work was partially funded by the Energy Laboratory of the University of Houston and by the Office of Naval Research.

[1] Q. Ouyang and H. L. Swinney, Chaos **1**, 411 (1991); Q. Ouyang and H. L. Swinney, Nature (London) **352**, 610 (1991).

[2] R. E. Rosensweig, J. Magn. Magn. Mater. **39**, 127 (1983).

[3] D. Sornette, J. Phys. (Paris) **48**, 151 (1987); C. Kooy and U. Enz, Philips Res. Rep. **15**, 7 (1960); P. Molho, J. Gouzerh, J. C. S. Levy, and J. L. Porteseil, J. Magn. Magn. Mater. **54**, 857 (1987); K. L. Babcock and R. M. Westervelt, Phys. Rev. A **40**, 2022 (1989).

[4] B. Dionne and M. Golubitsky, Z. Angew Math. Phys. **43**, 36 (1992).

[5] $U(\mathbf{x},t)$ being a real variable is the real part of the right side of (1).

[6] A. C. Newell and J. A. Whitehead, J. Fluid. Mech. **38**, 279 (1969); L. A. Segel, J. Fluid. Mech. **38**, 203 (1969).

[7] E. Buzano and M. Golubitsky, Philos. Trans. R. Soc. London A **308**, 617 (1983).

[8] S. Ciliberto, P. Coullet, J. Lega, E. Pampaloni, and C. Perez-Garcia, Phys. Rev. Lett. **65**, 2370 (1990).

[9] M. S. Heutmaker and J. P. Gollub, Phys. Rev. A **35**, 242 (1987).

[10] H. R. Brand, P. S. Lomdahl, and A. C. Newell, Physica (Amsterdam) **23D**, 345 (1986).

[11] A. C. Newell, in *Lectures in the Sciences of Complexity,* edited by D. L. Stein (Addison-Wesley, Reading, MA, 1989); A. C. Newell, T. Passot, and J. Lega, Annu. Rev. Fluid Mech. **25**, 399 (1993).

[12] $U(\mathcal{R}^{-1}\mathbf{x},t)=\sum A_n(\mathcal{R}^{-1}\mathbf{x},t)e^{i\mathbf{k}_n\cdot(\mathcal{R}^{-1}\mathbf{x})}=\sum A_n(\mathcal{R}^{-1}\mathbf{x},t)\times e^{i(\mathcal{R}\mathbf{k}_n)\cdot\mathbf{x}}=\sum[A_n(\mathcal{R}^{-1}\mathbf{x},t)e^{i\Delta\mathbf{k}_n\cdot\mathbf{x}}]e^{i\mathbf{k}_n\cdot\mathbf{x}}$.

[13] Q. Ouyang, G. H. Gunaratne, and H. L. Swinney, "Formation of Rhombic Patterns," University of Texas report (to be published).

[14] V. Dufiet and J. Boissonade, J. Chem. Phys. **96**, 664 (1992).

[15] H. R. Brand, Prog. Theor. Phys. Suppl. **99**, 442 (1989).

[16] W. H. Press, B. P. Flannery, S. A. Teukolsky, and W. T. Vettering, *Numerical Recipes—The Art of Scientific Computing* (Cambridge Univ. Press, Cambridge, 1988).

[17] The fluctuations decrease on decreasing the time step δt.

[18] In the Cross-Newell model [M. C. Cross and A. C. Newell, Physica (Amsterdam) **10D**, 299 (1984)] neighboring domains can be shown to prefer to be at an angle 120° from each other. We thank A. C. Newell for pointing this out.

[19] Y. Tu and M. C. Cross, Phys. Rev. Lett. **69**, 2515 (1992); B. A. Malomed, A. A. Nepomnyashchy, and M. I. Tribelsky, Phys. Rev. A **42**, 7244 (1990).

FIG. 2. A *chemically turbulent* pattern from the CIMA reaction (Ouyang and Swinney). The dark (light) regions of the figure correspond to the reduced (oxidized) states of the system.